MADRID
inter.noise 2019
June 16 - 19
NOISE CONTROL FOR A BETTER ENVIRONMENT

# Effect of frequency-dependent ground impedance on the sound pressure level of a moving source

**Mansour Alkmim**[1], **Laurent De Ryck, Jacques Cuenca**
**Siemens Industry Software**
**Interleuvenlaan 68, B-3001 Leuven, Belgium**

## ABSTRACT

**Analytical and numerical models for sound propagation within a bounded domain are commonly developed in the frequency domain. Time-domain models, however, are an interesting alternative when studying transient effects, non-uniform motion and for auralization purposes. Recent developments have been proposed to include the effect of time-domain locally-reacting impedance into the pressure field solution. While the direct wave frequency for harmonic source remains unmodified, the frequency of the acoustic wave reflecting on the ground is modified due to the source motion. This work proposes a study of the influence of different ground models in the sound propagation from a moving monopolar source. The model relies on the transient time delayed Green's function formulation which extends the result of classical Doppler Weyl-Van der Pol equation for arbitrary velocity. The wave reflecting on the ground is accounted for using an image source with its amplitude attenuated according to a dopplerised frequency ground impedance model. A comparative study is proposed and applications to real scenarios are presented.**

**Keywords:** ground impedance, moving monopole source, spherical reflection
**I-INCE Classification of Subject Number:** 30
(see http://i-ince.org/files/data/classification.pdf)

## 1. INTRODUCTION

Pavements are a major contributor of sound propagation in urban environments. Due to an ever increasing desire for noise reduction on roads, new tools have been created to characterize the acoustic behaviour of roads. Road noise is a complex phenomenon involving sound from different sources. For instance, tire-road interaction is closely dependent on the nature of the road surface, whereas wind noise and noise generated by the vehicle engine, power unit, exhaust are independent from the road properties. Despite

[1]mansour.alkmim@siemens.com

the absence of physical contact with the road, the perceived noise from the latter sources is still affected by road properties by means of sound reflection.

For this reason, the influence of ground impedance on outdoor sound propagation must not rely on a simplified classification of ground surfaces as soft or hard [1]. The acoustic properties of pavements present inherent features worthy of attention. For instance, porosity is very low compared with other typical acoustic materials [2]. Also, road properties can vary drastically with time. Small imperfections and damages to the road surface caused by different weather conditions make it challenging to model and characterize its properties.

Analytical and numerical models for sound propagation within a bounded domain are commonly developed in the frequency domain. However, time-domain models are an interesting alternative when studying transient effects, non-uniform motion and for auralization purposes. The advantage of a time-domain synthesis is that signals in the time domain enables directly sound quality analysis which has become more important with advances in electrical vehicles and the use of psychoacoustic metrics.

This paper deals with the influence of the influence of ground model properties on the sound propagation from a moving monopolar source. A common simplification of the multiple sources representing the car's component is to consider each component as a combination of monopole sources given that the source-receiver distance is sufficiently large to satisfy the far-field condition. This approach has been utilized in the audio source quantization in combination with a transfer path analysis [3].

The model relies on the transient time delayed Green's function formulation which extends the result of classical Doppler Weyl-Van der Pol equation for arbitrary velocity and on modelling of complex ground reflection by using an image source. First, a brief introduction of the mathematical formulation is presented. Then, a simulated example is shown considering the different scenarios focusing on the influence of the moving source on the variation of ground parameters.

## 2. ACOUSTIC RESPONSE OF A MOVING POINT SOURCE ABOVE A SOUND-ABSORBING SURFACE

In this section, the formulation of the acoustic field resulting from a point source with arbitrary speed and arbitrary trajectory moving above a frequency-dependent ground is presented. The geometry of the problem is shown in Fig. 1. The goal is to obtain the acoustic pressure at any fixed receiver position $\mathbf{r} = (x, y, z) \in \mathbb{R}^3$. The source position is denoted $\mathbf{r}_s(t) = (x_s(t), y_s(t), z_s(t)) \in \mathbb{R}^3$ with $t \in \mathbb{R}$. We begin with the solution of the pressure field in an unbounded domain then, later on, the effect of the ground is considered.

Consider the lossless scalar wave equation in an unbounded domain, the velocity potential $\varphi$ satisfies

$$\left(\nabla^2 - \frac{1}{c^2}\frac{\partial^2}{\partial t^2}\right)\varphi(\mathbf{r}, t) = -S(\mathbf{r}, t), \tag{1}$$

where $c$ is the speed of sound, $\nabla$ is the partial spatial derivative operator and $S(\mathbf{r}, t) = s(t)\delta[\mathbf{r} - \mathbf{r}_s(t)]$ is the source distribution density, $\delta[\mathbf{r} - \mathbf{r}_s(t)]$ is the 3D Dirac distribution and $s(t)$ is the source strength (or signature). It follows that the velocity potential can be

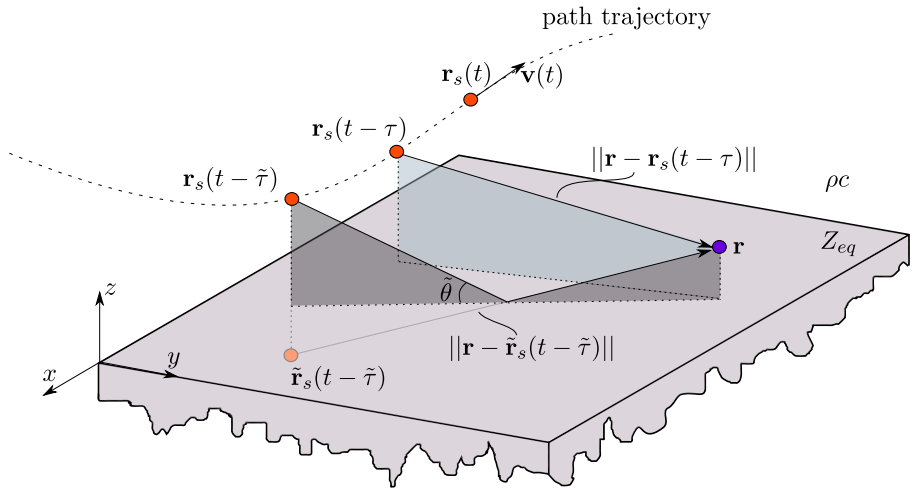


*Figure 1: Non-uniform non-rectilinear monopole source motion described by $\boldsymbol{r}_s(t)$ and $\boldsymbol{v}(t)$. The source emits pulses at a certain rate which propagate through the medium. The first direct pulse to hit the receiver at instant $t$ was emitted at time $t-\tau$ and the first reflected pulse was emitted at $t-\tilde{\tau}$ where $\tau$ and $\tilde{\tau}$ are the time delay for the direct and reflected pressure wave respectively.*

obtained by means of a time convolution operation as [4]

$$\varphi(\mathbf{r},t)=\frac{s(t-\tau)}{4\pi\|\mathbf{r}-\mathbf{r}_s(t-\tau)\|-\left[\dfrac{1}{c}\mathbf{v}(t-\tau)\cdot(\mathbf{r}-\mathbf{r}_s(t-\tau))\right]}, \tag{2}$$

where $\mathbf{v}$ is the source velocity and $s(t-\tau)$ is the delayed source signal, where time delay $\tau$ which can be obtained by the following implicit relation

$$\tau(\mathbf{r},t)=\frac{\|\mathbf{r}-\mathbf{r}_s(t-\tau)\|}{c}. \tag{3}$$

Differentiating Eq.(2) with respect to time, we can retrieve the pressure field as

$$p(\mathbf{r},t)=\frac{1}{4\pi}\left\{\frac{\dot{s}(t-\tau)R(t)}{\left[R(t)-\dfrac{1}{c}\mathbf{v}(t-\tau)\cdot\mathbf{R}(t)\right]^2}\right.$$
$$\left.+\frac{s(t-\tau)R(t)}{\left[R(t)-\dfrac{1}{c}\mathbf{v}(t-\tau)\cdot\mathbf{R}(t)\right]^3}\left(\frac{\mathbf{v}(t-\tau)\cdot\mathbf{R}(t)}{R(t)}+\frac{\mathbf{a}(t-\tau)\cdot\mathbf{R}(t)}{c}+\frac{[\mathbf{v}(t-\tau)]^2}{c}\right)\right\}, \tag{4}$$

where the shorthand notation $\mathbf{R}(t)=\mathbf{r}-\mathbf{r}_s(t-\tau)$ is used and $R=|\mathbf{R}|$. Note that except for a sign difference on the last term, Eq. (4) is the one obtained in Ref. [5].

For the arbitrary velocity case, the exact solution for the propagation time delay in Eq. (3) cannot be obtained explicitly since the nonlinear relation requires the prior knowledge of the position at current delay. For this reason a numerical approximation is employed considering the first-order Taylor expansion [6]

$$\tau(\mathbf{r},t+dt)\approx\tau(\mathbf{r},t)+dt\frac{d\tau(\mathbf{r},t)}{dt}, \tag{5}$$

### 2.2.1. Moving source with uniform velocity

Assuming the source is moving along the $x$-axis, the source position is given by $\mathbf{r}_s(t) = (x_0 + v_x t, 0, 0)$, with initial position $x_0$ and constant source velocity $v_x$. Eq. (4) reduces to the classical Doppler Weyl-Van der Pol equation [7]

$$p(\mathbf{r}, t) = \frac{1}{4\pi}\left\{\frac{\dot{s}(t-\tau)R}{[R(1 - M_x\cos\vartheta)]^2} + \frac{s(t-\tau)Rv(\cos\vartheta + M_x)}{[R(1 - M_x\cos\vartheta)]^3}\right\}, \tag{6}$$

where $\vartheta$ is the angle between the velocity vector $\mathbf{v}$ and the source-receiver distance vector $\mathbf{R}$. Note that the Mach number $M_x = v_x/c$ is time-invariant.

In this simple case, an analytical expression for the time propagation delay is given by

$$\tau = \frac{M_x(x - v_x t) + \sqrt{(x - v_x t)^2 + (y^2 + z^2)(1 - M_x^2)}}{c(1 - M_x^2)}, \tag{7}$$

### 2.2.2. Moving source above a frequency-dependent ground impedance

Equation (4) describes the pressure field of a moving source for an unbounded domain. In order to consider the effect of the ground, the boundary conditions must be satisfied. At each receiver location, the direct and reflected fields superpose, with the latter accounting for the complex dopplerised frequency-dependent surface impedance $Z$. This assumes a locally-reacting ground [8, 9].

For a bounded domain, we introduce the reflected field as resulting from an image source. Furthermore, by considering the correction for spherical waves [10] as a reflection operator $q$, we can describe the total pressure field in the time domain as the superposition of the direct and reflected fields as

$$p_{total}(\mathbf{r}, t) = p(\mathbf{r}, t) + q(t) * \tilde{p}(\mathbf{r}, t), \tag{8}$$

where $q(t) = \Im^{-1}\{Q(\tilde{\omega})\}$ is the inverse Fourier transform operator of the spherical wave reflection coefficient and $\tilde{p}(\mathbf{r}, t) \equiv p([\mathbf{r}|\tilde{\mathbf{r}}_s(t - \tilde{\tau})], t)$ is calculated considering the virtual source $\tilde{\mathbf{r}}_s(t - \tilde{\tau})$ at each delayed instant time $\tilde{\tau}$. Notice that the image source's propagation time delay is not the same as the original source due to the difference in distance traveled by the direct and reflected pressure field. Accordingly, the propagation time delay from the image source is the one considered for the ground reflection analysis.

The spherical wave reflection formulation is an approximation by a uniform asymptotic expansion combining the steepest descent and pole subtraction method [11] and is given by $Q(\tilde{\omega}) = R_p(\tilde{\omega}) + [1 - R_p(\tilde{\omega})]F(\tilde{\varepsilon})$ where $F(\varepsilon)$ is the boundary loss factor, $\tilde{\varepsilon} = \varepsilon(\tilde{\omega})$ is the complex numerical distance and $\tilde{\omega}$ is the Doppler-corrected circular frequency given by [2]

$$F(\tilde{\varepsilon}) = 1 + j\sqrt{\pi}\tilde{\varepsilon}\exp(-\tilde{\varepsilon}^2)\mathrm{erfc}(-j\tilde{\varepsilon}) \tag{9}$$

$$\varepsilon^2(\tilde{\omega}) = 2jk_0\chi^2(\tilde{\omega})\frac{\|\mathbf{r} - \tilde{\mathbf{r}}_s(t - \tilde{\tau})\|}{Z(\tilde{\omega})\left[1 - R_p(\tilde{\omega})\right]^2} \tag{10}$$

$$\tilde{\omega} = \omega\frac{R(t)}{[R(t) - \mathbf{M}(t - \tau)\cdot\mathbf{R}(t)]}, \tag{11}$$

where the term multiplying the circular frequency in Eq.11 is known as the Doppler factor.

The plane wave reflection of a moving source is defined as $R_p(\tilde{\theta};\tilde{\omega})$ which is calculated at the emission time of the reflected wave and depends on the angle of incidence $\tilde{\theta} = \theta(t-\tau)$ calculated at emission time

$$R_p(\tilde{\theta};\tilde{\omega}) = \frac{Z(\tilde{\omega})\sin\tilde{\theta} - \chi(\tilde{\omega})}{Z(\tilde{\omega})\sin\tilde{\theta} + \chi(\tilde{\omega})}, \tag{12}$$

where $Z(\tilde{\omega}) \equiv Z_{eq}(\Upsilon;\tilde{\omega})/\rho c$ is the frequency-dependent equivalent impedance and $Z_{eq}(\Upsilon;\tilde{\omega})$ is the characteristic ground impedance. The parameter $\Upsilon$ represents the ground properties that vary depending on the model chosen and the parameter $\chi$ is given by

$$\chi(\tilde{\omega}) = \sqrt{1 - \left(\frac{k_0}{k}\right)^2 \cos^2\tilde{\theta}}, \tag{13}$$

where $k_0 = \tilde{\omega}/c$ is the wavenumber in air. Note that the impedance models can account for different physical phenomena, and therefore a direct comparison is not attempted. Instead, the influence of individual parameters on the excess attenuation by the ground is investigated hereafter. The chosen ground model for this analysis is the Hamet model which is a three-parameter phenomenological model commonly used to characterize road pavements [12] and is described in frequency domain by its equivalent density and bulk modulus as follows

$$\tilde{\rho}_{eq}(\omega) = \frac{\rho K}{\phi}\left(1 - j\frac{\omega_\mu}{\omega}\right) \tag{14}$$

$$\tilde{K}_{eq}(\omega) = \frac{\rho c^2}{\phi}\frac{1}{1-(1-1/\gamma)/(1-j\omega_\theta/\omega)} \tag{15}$$

with

$$\omega_\theta = \frac{\sigma}{\rho Pr}, \quad \omega_\mu = \frac{\sigma\phi}{\rho K} \tag{16}$$

where $\rho$ is the air density, $Pr = 0.71$ is the Prandtl number for air at room temperature and $\gamma = 1.4$ is the air heat capacity ratio. The ground parameters are the porosity $\phi$, the shape factor (or structure factor) $K$ and the flow resistivity $\sigma$.

One can obtain the characteristic ground impedance and ground wave number as follows

$$Z_{eq} = \sqrt{\tilde{\rho}_{eq}\tilde{K}_{eq}}, \qquad k = \omega\sqrt{\tilde{\rho}_{eq}/\tilde{K}_{eq}}. \tag{17}$$

The transformation of such a frequency-dependent model to time-domain is not trivial due to the causality and stability of the system, for which certain conditions must be verified. Dragna et. al [13] investigated the admissibility of rigidly backed layers described by a surface impedance of the square-root family such as the Hamet model, where they showed its physical admissibility for time-domain transformation.

## 3. SIMULATED MOVING SOURCE IN A PASS-BY-NOISE SCENARIO

In this section we simulate different cinematic conditions of a moving source above a frequency-dependent ground and we evaluate the sensitivity of the model to the ground parameters. In this example, we consider that the point source is moving according to

a standard pass-by noise test. The source emits only single harmonic frequencies for simplicity. The receiver is located at the fixed position $\mathbf{r} = (x_{mid}, 7.5, 1.2)$ m, where the $x$-axis receiver position is at middle position and hence, it depends on the cinematic condition considered. The source is moving in a straight path with constant or accelerating speed $\mathbf{r}_s(t) = [v_x t + (1/2)a_x t^2, 0.0, 0.5]$ m, where $a_x$ is the acceleration in the $x$-axis. The parameters for the Hamet ground model were chosen arbitrarily: $\phi = 0.1$, $K = 10$, $\sigma = 10^5$ kPa $\cdot$ s $\cdot$ m$^{-2}$.

The ground reflection can be evaluated by means of the instantaneous sound pressure level (SPL) and the instantaneous excess attenuation (IEA). The definition of instantaneous sound pressure level is [14]

$$\mathrm{SPL}(t) = 10 \log_{10} \frac{1}{\Delta t} \int_{\Delta t} \frac{p^2(t)}{p_0^2} dt. \tag{18}$$

The instantaneous excess attenuation is defined as the difference between the sound pressure level in a bounded domain and the sound pressure level in a free field condition. In other words, it measures how much the ground reflect impact the sound pressure level.

$$\mathrm{IEA}(t) = SPL - SPL_{ff} = 10 \log_{10} \frac{1}{\Delta t} \int_{\Delta t} \frac{p^2(t)}{p_{A,ff}^2(t)} dt \tag{19}$$

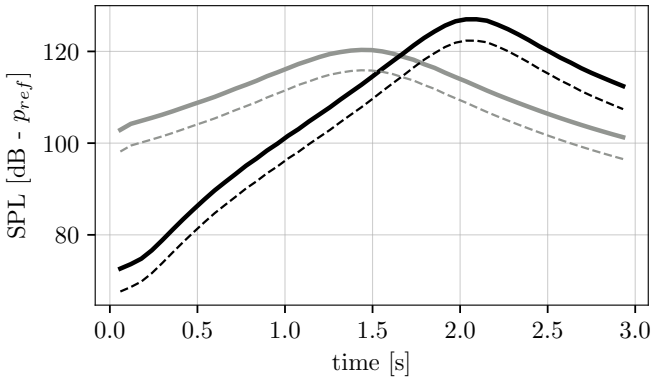


(a)

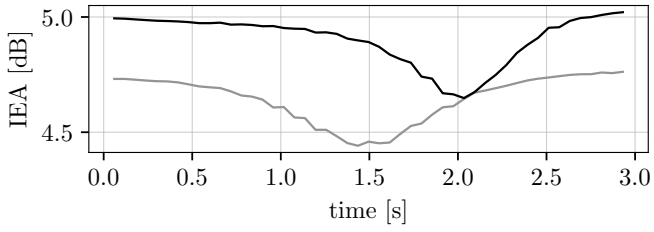


(b)

*Figure 2: SPL and EA for two cinematic conditions: (——) constant velocity $v_x = 14$ m $\cdot$ s$^{-1}$ and (——) accelerating $a_x = 10$ m $\cdot$ s$^{-2}$. The SPL without reflection for both cases is shown in dashed lines (- - - -). The source emits a harmonic signal at $f = 200$ Hz and the sample time is 3 s.*

In Fig. 2, two cinematic conditions are considered: constant velocity $v_x = 14$ m $\cdot$ s$^{-1}$ and accelerating $a_x = 10$ m $\cdot$ s$^{-2}$. The receiver is fixed at $\mathbf{r} = (21, 7.5, 1.2)$ m and

the source emits a single frequency signal at 200 Hz. Figure 2(a) shows the sound pressure level. A symmetric instantaneous sound pressure level can be seen for the constant velocity case with a peak when the source crosses the receiver position, which occurs at different times depending on the speed. For the accelerating case, the sound pressure level increases gradually and its peak value occurs 0.5 s later than the constant velocity case because the moving source takes longer to cross the receiver. In both cases the instantaneous sound pressure level without reflection is shown as dashed lines, the difference is constant through time and has a marginal effect of around 4 and 5 dB. This effect can be seen more clearly by analyzing the variation in instantaneous excess attenuation at Fig.2(b). For both cases, the ground reflection has a slightly variation of around 0.5 dB during simulated time of 3 s. Minimum excess attenuation occurs when there is a maximum sound pressure level, at this point the source and receiver are the closest and hence it has the smallest propagation path. At this instant, the ground reflection has minimum impact on the sound pressure level.

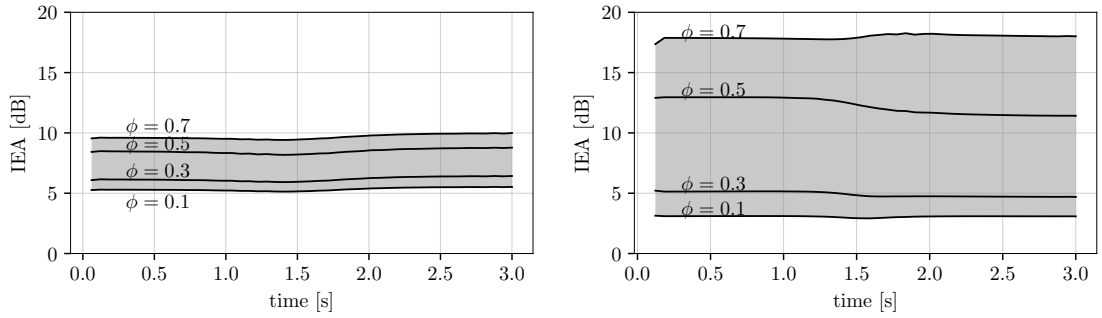


*Figure 3: Instantaneous excess attenuation of a moving source with constant velocity (a) $v = 14\ \mathrm{m \cdot s^{-1}}$ and (b) $v = 30\ \mathrm{m \cdot s^{-1}}$ for a range of porosities. Considering source emitting a harmonic signal at $f = 200$ Hz.*

Figure 3 shows the IEA to evaluate the sensitivity of the microstructural parameters to the variation in speed. The porosity remains nearly constant in time for both cinematic conditions. However, the increase in velocity increases the sensitivity of porosity with a variation ranging 15 dBs.

Figure 4 shows the minimum instantaneous excess attenuation at a certain position in time to the porosity variation with respect to the harmonic frequency the source emits. A minimum IEA means the position where the ground reflection has less impact on the SPL, in other words, the position where the ground has its highest absorption. The three cinematic conditions for the source are stationarity, constant velocity and constant acceleration. For the stationary case in Figure 4(a) the minimum IEA remains almost constant with frequency. In the two moving cases, below $f = 1$ kHz, the minimum IEA decreases with an increase in source emitting frequency but the porosity variation remains constant. After this point both the minimum IEA and porosity shows high sensitivity to the emitted frequency. Comparing the two moving source cases with the stationary case, it indicates that the porosity can vary due to the moving source and this variability increases for sources emitting higher frequencies.

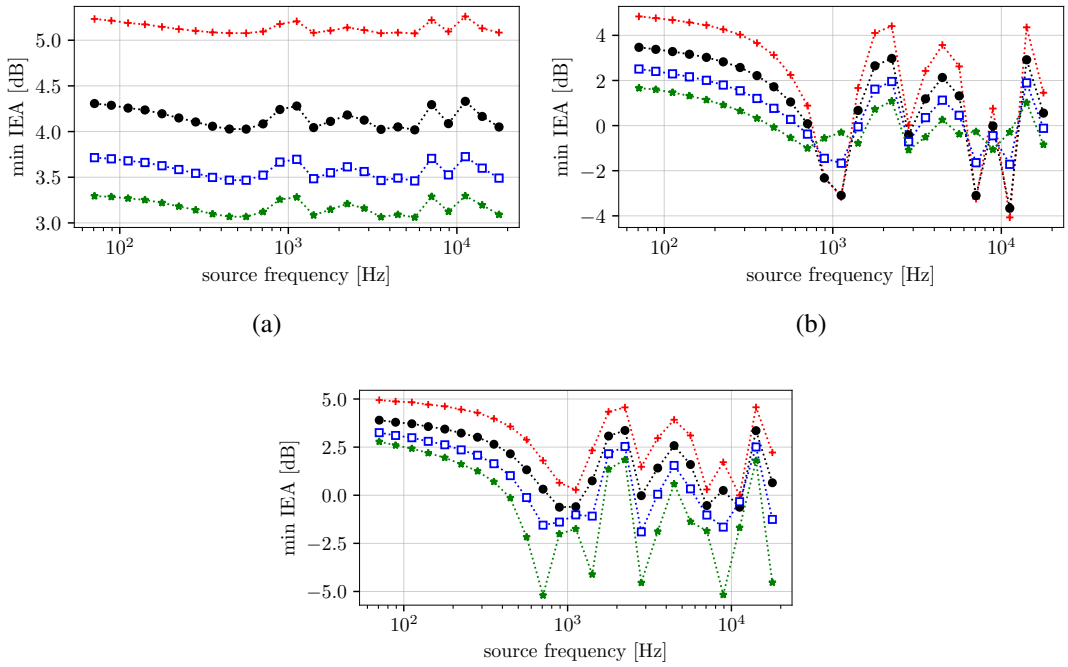


*Figure 4: Minimum instantaneous excess attenuation at the instant when the source is crossing the receiver for different harmonic source frequency (third octave bands) and different porosity: (··+·· $\phi = 0.1$), (··●·· $\phi = 0.3$), (··□·· $\phi = 0.5$), (··★·· $\phi = 0.7$) in three scenarios (a) stationary, (b) constant velocity $v = 14$ m/s and (c) constant acceleration $a = 10$ m/s$^2$.*

## 4. CONCLUSIONS

A formulation of the acoustic field resulting from a point source with arbitrary speed and arbitrary trajectory moving above a frequency-dependent ground is presented. The tool allows for different scenarios to be simulated, such as different geometries, paths, cinematic conditions, source signal and ground models. In this paper we investigated the effect of motion of a point source above ground considering Hamet impedance model. In the example given, the monopole source is simulated in a pass-by noise scenario. We first looked into the SPL and IEA for two cinematic conditions where the ground reflection showed little variation due to the moving source. This effect can be noticed more clearly when analyzing the IEA.

The second analysis concerned the influence of source speed into the ground porosity. Two velocities are simulated, for the low speed case the Doppler effect in the ground parameter exhibited slight variation of 5 dB. The effect of ground reflection increases as the source speed increases and the porosity showed higher variability to the cinematic conditions. This can be attributed to the increased effect of the Doppler effect. However, the transient effect of porosity is negligible. In the third and final analysis, we compared the minimum instantaneous excess attenuation at a certain position in time to the porosity variation with respect to the harmonic frequency the source emits. Results indicate that the sensitivity to porosity has a considerable variation due to the moving source and this variability can increase for sources emitting higher frequencies.

The analytical model demonstrates its potential for virtual pass-by-noise simulation

which can be use to assess acoustic properties of a moving source above different grounds. However, there are still challenges to be addressed such as the physical validity of the model against an experiment and the lack of tire-road interaction taking into account road models.

## 5. ACKNOWLEDGEMENTS

We gratefully acknowledge the European Commission for its support of the Marie Sklodowska Curie program through the H2020 ETN PBNv2 project (GA 721615).

## 6. REFERENCES

[1] Keith Attenborough, Imran Bashir, and Shahram Taherzadeh. Outdoor ground impedance models. *The Journal of the Acoustical Society of America*, 2011.

[2] Gaëlle Benoit, Christophe Heinkélé, and Emmanuel Gourdon. Characterizing a porous road pavement using surface impedance measurement: A guided numerical inversion procedure. *The Journal of the Acoustical Society of America*, 2013.

[3] Karl Janssens, Pieter Aarnoutse, Peter Gajdatsy, Laurent Britte, Filip Deblauwe, and Herman Van der Auweraer. Time-Domain Source Contribution Analysis Method for In-Room Pass-By Noise. In *SAE Technical Paper*, 2011.

[4] Adrianus T. de Hoop. Fields and waves excited by impulsive point sources in motion—The general 3D time-domain Doppler effect. *Wave Motion*, 2005.

[5] Cédric Camier, Jean-François Blais, Robby Lapointe, and Alain Berry. A time-domain analysis of 3D non-uniform moving acoustic sources: Application to source identification and absolute quantification via beamforming. In *Beamforming Berlin Conference 2012*, 2012.

[6] Gergely Firtha and Péter Fiala. Wave Field Synthesis of moving sources with arbitrary trajectory and velocity profile. *The Journal of the Acoustical Society of America*, 2017.

[7] Philip McCord Morse and K. Uno Ingard. *Theoretical Acoustics*. Princeton University Press, 1986.

[8] Marc Buret. *New Analytical Models for Outdoor Moving Sources of Sound*. Ph.D., Open University, 2002.

[9] D. Dragna and P. Blanc-Benon. Sound radiation by a moving line source above an impedance plane with frequency-dependent properties. *Journal of Sound and Vibration*, 2015.

[10] M C Berengier and B Gauvreau. Outdoor Sound Propagation: A Short Review on Analytical and Numerical Approaches. *Acta Acustica United With Acustica*, 2003.

[11] Keith Attenborough, Kai Ming Li, and Kirill Horoshenkov. *Predicting Outdoor Sound*. CRC Press, 2014.

[12] Jean-Francois Hamet and Michel Berengier. Acoustical characteristics of porous pavements: A new phenomenological model. In *Inter-Noise 93: People Versus Noise*, 1993.

[13] Didier Dragna and Philippe Blanc-Benon. Physically Admissible Impedance Models for Time-Domain Computations of Outdoor Sound Propagation. *Acta Acustica united with Acustica*, 2014.

[14] B.M. Favre and B.T. Gras. Noise emission of road vehicles: Reconstitution of the acoustic signature. *Journal of Sound and Vibration*, 1984.